*Journal of Experimental Botany, Vol. 59, No. 14, pp. 3845–3855, 2008*
doi:10.1093/jxb/ern225 Advance Access publication 1 October, 2008
This paper is available online free of all access charges (see http://jxb.oxfordjournals.org/open_access.html for further details)

Journal of Experimental Botany
www.jxb.oxfordjournals.org

**RESEARCH PAPER**

# Homeostatic control of slow vacuolar channels by luminal cations and evaluation of the channel-mediated tonoplast $Ca^{2+}$ fluxes *in situ*

**V. Pérez[1], T. Wherrett[2], S. Shabala[2], J. Muñiz[1], O. Dobrovinskaya[1] and I. Pottosin[1,*]**

[1] *Centro Universitario de Investigaciones Biomédicas. Universidad de Colima, 28045 Colima, Col., México*

[2] *School of Agricultural Science, University of Tasmania, Tas7001, Australia*

Received 12 June 2008; Revised 5 August 2008; Accepted 6 August 2008

## Abstract

**$Ca^{2+}$, $Mg^{2+}$, and $K^+$ activities in red beet (*Beta vulgaris* L.) vacuoles were evaluated using conventional ion-selective microelectrodes and, in the case of $Ca^{2+}$, by non-invasive ion flux measurements (MIFE) as well. The mean vacuolar $Ca^{2+}$ activity was ~0.2 mM. Modulation of the slow vacuolar (SV) channel voltage dependence by $Ca^{2+}$ in the absence and presence of other cations at their physiological concentrations was studied by patch-clamp in excised tonoplast patches. Lowering pH at the vacuolar side from 7.5 to 5.5 (at zero vacuolar $Ca^{2+}$) did not affect the channel voltage dependence, but abolished sensitivity to luminal $Ca^{2+}$ within a physiological range of concentrations (0.1–1.0 mM). Aggregation of the physiological vacuolar $Na^+$ (60 mM) and $Mg^{2+}$ (8 mM) concentrations also results in the SV channel becoming almost insensitive to vacuolar $Ca^{2+}$ variation in a range from nanomoles to 0.1 mM. At physiological cation concentrations at the vacuolar side, cytosolic $Ca^{2+}$ activates the SV channel in a voltage-independent manner with $K_d$=0.7–1.5 μM. Comparison of the vacuolar $Ca^{2+}$ fluxes measured by both the MIFE technique and from estimating the SV channel activity in attached patches, suggests that, at resting membrane potentials, even at elevated (20 μM) cytosolic $Ca^{2+}$, only 0.5% of SV channels are open. This mediates a $Ca^{2+}$ release of only a few pA per vacuole (~0.1 pA per single SV channel). Overall, our data suggest that the release of $Ca^{2+}$ through SV channels makes little contribution to a global cytosolic $Ca^{2+}$ signal.**

Key words: Calcium channel, calcium signalling, patch-clamp, SV channel, tonoplast, vacuole.

## Introduction

Slow vacuolar (SV) channels are ubiquitous in all tissues of higher plants with several thousand per vacuole (Hedrich *et al*., 1988; Schulz-Lessdorf and Hedrich, 1995; Pottosin *et al*., 1997). The SV channel is a non-selective cation channel with significant $Ca^{2+}$ permeability (Ward and Schroeder, 1994; Gradmann *et al*., 1997; Allen *et al*., 1998; Pottosin *et al*., 2001), encoded by the TPC1 (two-pore calcium channel) singleton gene (Peiter *et al*., 2005). The SV channel is undoubtedly the best explored and the most abundant vacuolar channel, as shown by electrophysiological and proteomics studies of the tonoplast (Schulz-Lessdorf and Hedrich, 1995; Carter *et al*., 2004; Pottosin and Schönknecht, 2007).

Because the vacuole is the largest $Ca^{2+}$ store in plant cells, there is an ongoing debate as to the level of participation of the SV channel in $Ca^{2+}$ signalling. For instance, based on the finding that the SV channel is activated by increased cytosolic $Ca^{2+}$, Ward and Schroeder (1994) proposed that these channels take part in the so-called CICR ($Ca^{2+}$-induced $Ca^{2+}$ release), a potentiation of the initial $Ca^{2+}$ signal. However, experiments with *tpc1*-knockout Arabidopsis plants did not reveal any clear changes in the phenotype, thus questioning the participation of the SV channel in $Ca^{2+}$ responses to a variety of stimuli (Peiter *et al*., 2005; Ranf *et al*., 2008).

Slow vacuolar channels are regulated by a variety of physiological factors (see Pottosin and Schönknecht,

* To whom correspondence should be addressed. E-mail: pottosin@ucol.mx

2007, for a recent review). Most pronounced are the activation by cytosolic $Ca^{2+}$ (Hedrich and Neher, 1987; Ward and Schroeder, 1994; Schulz-Lessdorf and Hedrich, 1995), and negative modulation by vacuolar $Ca^{2+}$ (Pottosin *et al*., 1997, 2004). In the first attempt to quantify the joint impact of luminal and cytosolic $Ca^{2+}$ on SV channel activity, Pottosin and co-workers (1997) demonstrated that the inhibitory effect of vacuolar $Ca^{2+}$ prevailed the channel stimulation by cytosolic $Ca^{2+}$. Hence, at realistic electrochemical $Ca^{2+}$ gradients across the tonoplast that favour $Ca^{2+}$ release from the vacuole, only a tiny fraction of SV channels is active.

However, while the range of cytosolic $Ca^{2+}$ variation is well established, all the information regarding the free vacuolar $Ca^{2+}$ in higher plants comes essentially from a single study (Felle, 1988). In the absence of $Ca^{2+}$, other vacuolar cations increase the threshold for the SV channel voltage activation, specifically in the case of $Mg^{2+}$, $Na^{+}$, and $Cs^{+}$, or non-specifically via screening of the negative surface charge ($K^{+}$, choline, NMDG) (Pottosin *et al*., 2004, 2005; Ivashikina and Hedrich, 2005; Ranf *et al*., 2008). Furthermore, the effects of different vacuolar cations were not additive. For instance, at zero vacuolar $Ca^{2+}$, increases in the vacuolar $K^{+}$ caused a *positive* shift of SV channel voltage dependence, whereas at 0.5 mM vacuolar $Ca^{2+}$, the same increase in vacuolar $K^{+}$ caused a *negative* shift (Pottosin *et al*., 2005). Also, cytosolic $Mg^{2+}$, especially at low cytosolic $Ca^{2+}$, acted as a positive regulator of the SV channel (Pei *et al*., 1999; Carpaneto *et al*., 2001). Consequently, the free concentrations of physiologically abundant vacuolar cations such as $Na^{+}$, $K^{+}$, $Ca^{2+}$, and $Mg^{2+}$, remain to be determined and their joint effect on the SV channel voltage dependence, evaluated.

In light of this, the vacuolar levels of these cations were measured and these values were used to quantify the SV channel activity under a physiological range of cytosolic $Ca^{2+}$ and $Mg^{2+}$ activities. This was then compared with the SV channel activity measured *in situ* from attached patches and with $Ca^{2+}$ fluxes measured on isolated vacuoles using the MIFE technique. Our results suggest that SV channel mediation of $Ca^{2+}$ release from the vacuole is insufficient to support global $Ca^{2+}$ responses in higher plant cells.

## Materials and methods

### *Preparation*

Vacuoles were isolated mechanically from *Beta vulgaris* L. taproot slices as described previously (Pottosin *et al*., 2001). Briefly, sections of a taproot were soaked for at least 20 min in a solution essentially identical to the bath solution used in patch-clamp experiments, but made slightly (by 30–40 mOsm) hypertonic. Sections were cut with preparation needles under stereoscopic control, and vacuoles released were collected with a micropipette and transported to the experimental chamber.

### *Intravacuolar cation activities measurements*

Ion-selective microelectrodes for the determination of intravacuolar activities of $Ca^{2+}$, $Mg^{2+}$, and $K^{+}$ were fabricated from 1.5 mm non-filamented borosilicate glass capillaries (GC 150–10, CDR Clinical Technology, Middle Cove, Australia) pulled to the smallest diameter (<1 μm) that still allowed backfilling. Blank capillaries were oven-dried at 225 °C overnight. They were then covered with a steel lid for 10–15 min, before 40–50 μl tributylchlorosilane (90796, Fluka Chemicals) was injected under the lid, and the lid removed 10 min later. Electrode blanks were baked for a further 40 min to ensure complete drying, and allowed to cool before storage in a closed container for up to 6 weeks.

Micropipettes were backfilled with the appropriate solution (Table 1) using a syringe with a thin metal needle. Filling with the ionophore (liquid ion exchanger, LIX) was performed immediately after backfilling by dipping the microelectrode into a wider tipped (30–50 μm) pulled capillary, filled by its submersion in the LIX stock solution. The LIX column obtained in the microelectrode tip was 100–200 μm long. Because the ion-selective microelectrode readings are affected by the ionic strength of the solutions, the activities of major osmotics ($K^{+}$, $Na^{+}$) were determined first, and calibration solutions were prepared accordingly.

Potassium electrodes were calibrated in a background of 60 mM NaCl and $Ca^{2+}$-electrode calibration solutions included 115 mM KCl and 60 mM NaCl. The changes in $Ca^{2+}$ activity between 150 μM and 350 μM, mimicking the variation in measured vacuolar $Ca^{2+}$, did not affect the electric potential values reported by $Mg^{2+}$-electrodes, so no additional corrections for $Ca^{2+}$ were made.

Microelectrode calibration was performed before and after impalement. Electrodes with slopes less than 50 mV (for $K^{+}$) or 25 mV per decade (for $Ca^{2+}$, $Mg^{2+}$), or a correlation coefficient less than 0.999, were discarded. Typical resistance of the microelectrodes was 1–3 GΩ. Measured microelectrodes voltages were corrected for potential values across the tonoplast and the liquid junction potentials (in mV: 1.3 for the $Ca^{2+}$-microelectrode, 1.4 for the $K^{+}$-microelectrode, and 6.6 for the $Mg^{2+}$-microelectrode). Results of trans-tonoplast electric potential difference, measured in a separate set of experiments with a glass microelectrode filled with 3 M KCl to minimize the liquid junction potentials, were used to correct potentials values reported by the ion-selective microelectrodes. The bath solution was 100 mM KCl, 1 mM HEPES (pH 7.4/KOH), adjusted with sorbitol to be slightly more hyperosmotic than the measured osmolality values for squeezed beet juice (500–650 mOsm).

Due to the low selectivity of the $Na^{+}$-LIX against $K^{+}$ and difficulties with front-filling $H^{+}$-LIX electrodes impalements, $Na^{+}$ and $H^{+}$ free activities could not be measured with ion-selective microelectrodes. Instead, centrifuged squeezed juice (mainly vacuolar sap) from beet taproots was used to measure the $Na^{+}$ concentration using a flame photometer, and $H^{+}$ activity, with conventional pH-electrodes.

**Table 1.** *Liquid ionophores and respective backfilling solutions used for ion selective microelectrodes*

| Ion | Liquid ion exchanger (LIX) | Backfilling solution |
|---|---|---|
| $Ca^{2+}$ | Calcium ionophore I — cocktail A (Sigma I-1772) | 500 mM $CaCl_2$ |
| $Mg^{2+}$ | Magnesium ionophore I — cocktail A (Fluka 63048) | 500 mM $MgCl_2$ |
| $K^{+}$ | Pottasium ionophore I — cocktail A (Fluka 60031) | 500 mM KCl |

### *$Ca^{2+}$ flux measurements with the MIFE technique*

$Ca^{2+}$-fluxes from *Beta* vacuoles were quantified using the Microelectrode Ion Flux Estimation (MIFE) technique (see Newman, 2001, for details and theoretical background). Microelectrodes fabricated for MIFE were similar to those used for vacuole impalements, except the tip diameter was 2–3 μm and drying time after silanization was 30 min.

Calibration of $Ca^{2+}$-selective MIFE-electrodes was performed in a background of 100 mM $K^+$. MIFE set-up and experimental procedure was essentially as described previously (Wherrett *et al*., 2005). The MIFE electrode was positioned at a distance of 10 μm from the vacuole surface and moved back and forth 50 μm horizontally to avoid the influence of ion leakage fluxes from the underlying glass chamber. Calcium fluxes were calculated by subtracting the background flux determined in the immediate proximity to the vacuole from the measured integral flux, taking into account the diameter of each analysed vacuole. $Ca^{2+}$-fluxes were estimated against a background of 100 mM KCl, 1 mM HEPES (pH 7.4 with KOH), and either 0, 20, 50, 70, 100, 150, or 250 μM $Ca^{2+}$, without $Ca^{2+}$-buffering (background $Ca^{2+}$-contamination was ~2 μM, as reported by $Ca^{2+}$-selective electrodes). The statistical significance of $Ca^{2+}$-flux changes under treatment with $Mg^{2+}$ and $Zn^{2+}$ was evaluated by a one way analysis of variance using SPSS, and mean comparison using Duncan's multiple range test.

### *Patch-clamp protocols and analyses*

Patch pipettes fabrication, patch-clamp set-up, and record acquisition and analyses were as described previously (Pottosin *et al*., 2001). The osmolality of all solutions was adjusted by sorbitol to isotonic levels with respect to the vacuolar sap (range 520–680 mOsm), verified using a cryoscopic osmometer (OSMOMAT 030, Gonotec, Germany).

The effects of the major vacuolar cations were examined in a set of experiments on excised patches with 100 mM KCl, 2 mM $CaCl_2$, 10 mM HEPES, pH 7.5, (with KOH) at the cytosolic side, and either 100 mM, 125 or 187 mM KCl, 0 or 62 mM NaCl, 0 or 8 mM $MgCl_2$, with a variable free $Ca^{2+}$ (0, 0.01, 0.05, 0.1, 0.2, 0.5, 1.0, 2.0 or 10.0 mM), 10 mM MES/KOH (pH 5.5 or 6.4), at the vacuolar side. For measurements in vacuole-attached configuration, patch pipettes were filled with the same cytosolic solution as above, while the bath contained 100 mM KCl, and 0, 0.05, 0.1, 0.2, 0.5, 1, 2 or 10 mM $Ca^{2+}$, 10 mM HEPES-KOH (pH 7.5). Voltages were corrected for the trans-tonoplast potential from values measured with a 3 M KCl-filled microelectrode in bath solutions containing the same free $Ca^{2+}$ concentration.

SV currents in vacuole-attached patches and small right-oriented (cytosolic side out) vacuolar vesicles were also analysed at ionic conditions mimicking the physiological cation concentrations. The vacuolar solution used was in mM: 125 $K^+$, 62 $Na^+$, 8 $Mg^{2+}$, 0.25 $Ca^{2+}$, pH 5.5 (MES/KOH), and the cytosolic solution contained: 100 mM $K^+$, 10 mM HEPES/KOH (pH 7.5) and 0.1, 1.0, 7.0 or 20 μM free $Ca^{2+}$, supplemented with either 0.5 or 1.5 mM free $Mg^{2+}$. Solutions with a certain free $Ca^{2+}$ and $Mg^{2+}$ concentrations were prepared using a combination of chelating agents (2 mM of EGTA, EDTA, HEDTA, and/or NTA). The free divalent cation concentration for each condition were calculated on the basis of their total concentration and concentrations of added chelating agents including ATP, taking into the account the ambient pH, temperature and ionic strength (WinMAXC[32] v.2.50, Chris Patton, Stanford University).

SV channel currents were evoked by a series of positive voltage steps from a holding potential of –100 mV (cytosol minus vacuole) or –20 mV (in experiments with low cytosolic $Ca^{2+}$), up to +200 mV in 20 mV increments. Unitary current–voltage (*I*/*V*) relationships at different ionic conditions and patch configurations were obtained by the application of 15 ms voltage-ramps between +200 and −200 mV as previously described (Pottosin *et al*., 2001). The SV activation curve (number or relative number of open channels versus trans-tonoplast electric potential difference) was obtained as described in detail by Pottosin *et al*. (2005). To describe the shift of the voltage dependence by vacuolar $Ca^{2+}$, a threshold voltage value ($V_{1\%}$), i.e. the voltage at which 1% of maximal SV channel activity was reached ($P/P_{max}$=0.01), was estimated at each given condition. Non-linear regression fitting of the data was performed using the GraFit v.6 data analysis and graphics program (Erithacus Software, Ltd).

## Results

### *Vacuolar $Ca^{2+}$ fluxes and cation concentrations*

One of the primary aims of this study was to evaluate net $Ca^{2+}$ release from sugar beet vacuoles. As one possible route of $Ca^{2+}$ escape from vacuoles are $Ca^{2+}$-activated SV channels, by applying the MIFE technique $Ca^{2+}$ flux measurements were performed at different levels of cytosolic (bath) $Ca^{2+}$ (Fig. 1A). However, the minimal $Ca^{2+}$ free concentration achieved was ~2 μM (reflecting contamination of the bath solution by the vacuolar isolation procedure) due to the inability of the MIFE technique to estimate net $Ca^{2+}$ fluxes in the presence of $Ca^{2+}$ buffers. This concentration is referred to as the 'trace bath $Ca^{2+}$' when referring to MIFE results. Under such minimal conditions, the net $Ca^{2+}$ release from vacuoles was close to the detection limit of the method (~1 nmol $m^{-2}$ $s^{-1}$). This flux tripled and reached its maximum at ~20 μM free $Ca^{2+}$ in the bath, while further increases in the free cytosolic $Ca^{2+}$ caused a gradual decrease of $Ca^{2+}$ flux, until it reversed polarity at ~200 μM cytosolic $Ca^{2+}$. This non-monotonic behaviour is consistent with passive $Ca^{2+}$ transport, mediated by some (presumably SV) $Ca^{2+}$-permeable channel, activated by cytosolic $Ca^{2+}$. Moreover, the observed $Ca^{2+}$ flux was significantly ($P < 0.05$) enhanced by 1.5 mM $Mg^{2+}$ and strongly suppressed by 0.1 mM $Zn^{2+}$ (Fig. 1B), known activator and blocker, respectively, of SV channels (Hedrich and Kurkdjian, 1988; Gambale *et al*., 1993; Pei *et al*., 1999; Carpaneto *et al*., 2001).

The SV channel is controlled by different mono and divalent cations present at cytosolic and vacuolar sides of the tonoplast. Therefore, to link the vacuolar $Ca^{2+}$ flux to the SV channel activity, a further attempt was made to evaluate the activities of physiologically relevant vacuolar cations. Because single-barrelled electrodes were used to determine the activities of $Ca^{2+}$, $Mg^{2+}$, and $K^+$ in fresh isolated sugar beet vacuoles (see Materials and methods for details), electrode readings were corrected for trans-tonoplast electric potential difference with measurements from a separate set of experiments using 3 M KCl-filled microelectrodes (Fig. 1C). However, due to the poor selectivity of all available $Na^+$ resins (Chen *et al*., 2005),

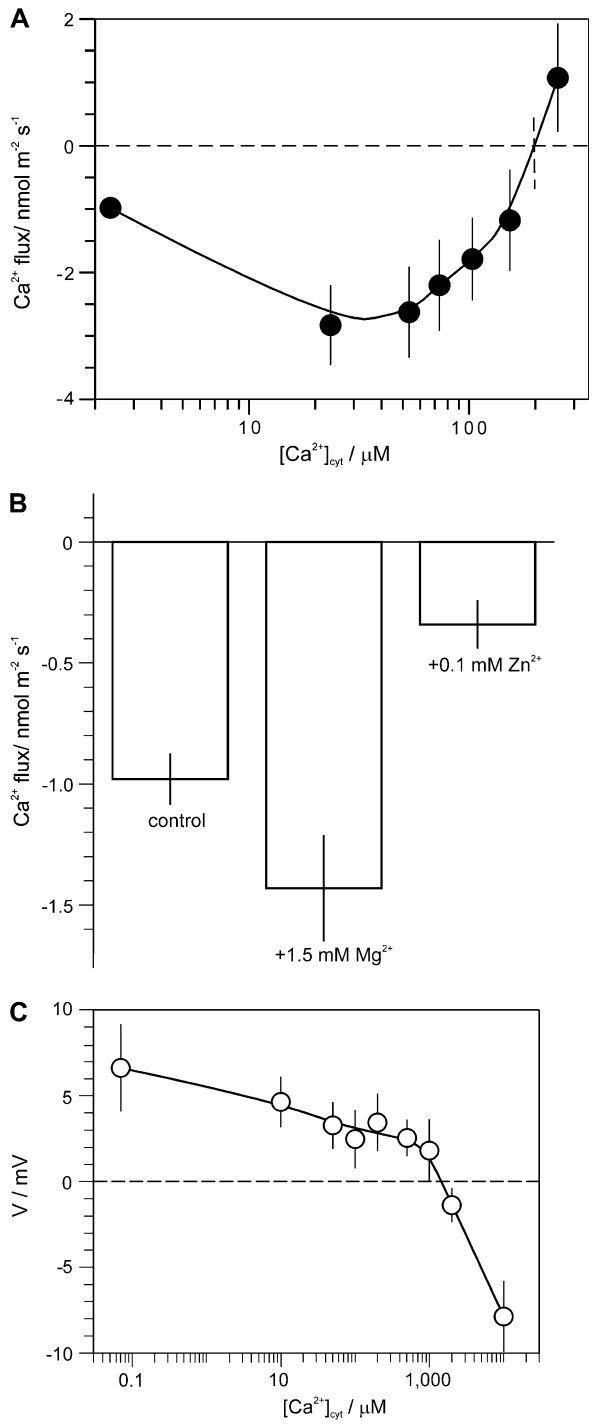


**Fig. 1.** Effects of cytosolic $Ca^{2+}$ on trans-tonoplast $Ca^{2+}$ fluxes and the membrane potential difference in isolated red beet vacuoles. (A) $Ca^{2+}$ fluxes from individual vacuoles measured with the MIFE technique ($n$=6–19 vacuoles for each $Ca^{2+}$ concentration in the bath). Negative flux implies a net $Ca^{2+}$ transport from the vacuole to the extravacuolar (cytosolic) side. (B) Vacuolar $Ca^{2+}$ flux stimulation by cytosolic $Mg^{2+}$ and inhibition by $Zn^{2+}$ ($n$=8–10 vacuoles). (C) Electric potential difference across the tonoplast as a function of bath free $Ca^{2+}$ ($n$=8–11 vacuoles). All data are presented as mean ±SEM. Bath: 100 mM KCl, pH 7.5.

vacuolar $Na^+$ concentrations were measured using conventional flame photometry. The results of these measurements are summarized in Table 2. Notably, the $Ca^{2+}$ activity was an order of magnitude lower (Table 2) than previously reported for distinct higher plant preparations (Felle, 1988). Moreover, the same $Ca^{2+}$ activity value was independently estimated from the reversal condition (respective bath $Ca^{2+}$concentration) of the $Ca^{2+}$ flux reported by MIFE, assuming equilibrium conditions for $Ca^{2+}$ exchange across the tonoplast and correcting the data for the resting tonoplast potential.

### *Modulation of the SV channel voltage dependence by vacuolar cations*

Our previous study has demonstrated a very strong dependence of the SV channel activation threshold on vacuolar $Ca^{2+}$ (Pottosin *et al.*, 2004). However, the above study was performed at a non-physiological vacuolar pH (7.5), while the actual pH of the vacuolar sap is around 5.9±0.3 ($n$=11 separate preparations). Accordingly, in this work the $Ca^{2+}$ modulation of the SV channel voltage dependence has been analysed at more physiologically relevant vacuolar pH values (6.4 and 5.5, respectively). The summary of the activation curves at different vacuolar $Ca^{2+}$ levels and pH 5.5 is presented in Fig. 2A. To make a single-parameter comparison of the $Ca^{2+}$ dependence at different vacuolar pH values, the membrane potential values at which 1% of available SV channels are open ($V_{1\%}$; see Pottosin *et al.*, 2005, for a justification) have been estimated. This technical activation threshold was plotted as a function of the vacuolar free $Ca^{2+}$ (Fig. 2B). At vacuolar pH 7.5 within a range from 10 μM to 10 mM $Ca^{2+}$, the SV channel behaves as a 'super-$Ca^{2+}$' electrode. The curve $V_{1\%}$ versus the vacuolar free $Ca^{2+}$ has a slope of ~40 mV per 10-fold increase in $Ca^{2+}$ concentration (as compared to 29.5 mV for an ideal $Ca^{2+}$ electrode). This is because the SV channel is able to bind more than one $Ca^{2+}$ ion from the vacuolar side (Pottosin *et al.*, 2004). Lowering the vacuolar pH desensitizes the SV channel to the vacuolar $Ca^{2+}$ changes within a physiological range of $Ca^{2+}$ concentrations (0.1–1 mM). At the same time, lowering the vacuolar pH by itself does not affect the SV

**Table 2.** *Activities of physiological cations in red beet* (Beta vulgaris *L.*) *vacuoles*

| Ion | Activity (mM) | Method |
|---|---|---|
| $K^+$ | 116±2 ($n$=8) | $K^+$-selective microelectrodes |
| $Na^+$ | 62±5[a] ($n$=5) | Flame photometry |
| $Mg^{2+}$ | 8.3±0.7 ($n$=7) | $Mg^{2+}$-selective microelectrodes |
| $Ca^{2+}$ | 0.20±0.02 ($n$=7) | $Ca^{2+}$-selective microelectrodes |
| | 0.21 | MIFE estimate (see Fig. 1) |

[a] Concentration instead of activity was determined in this case.

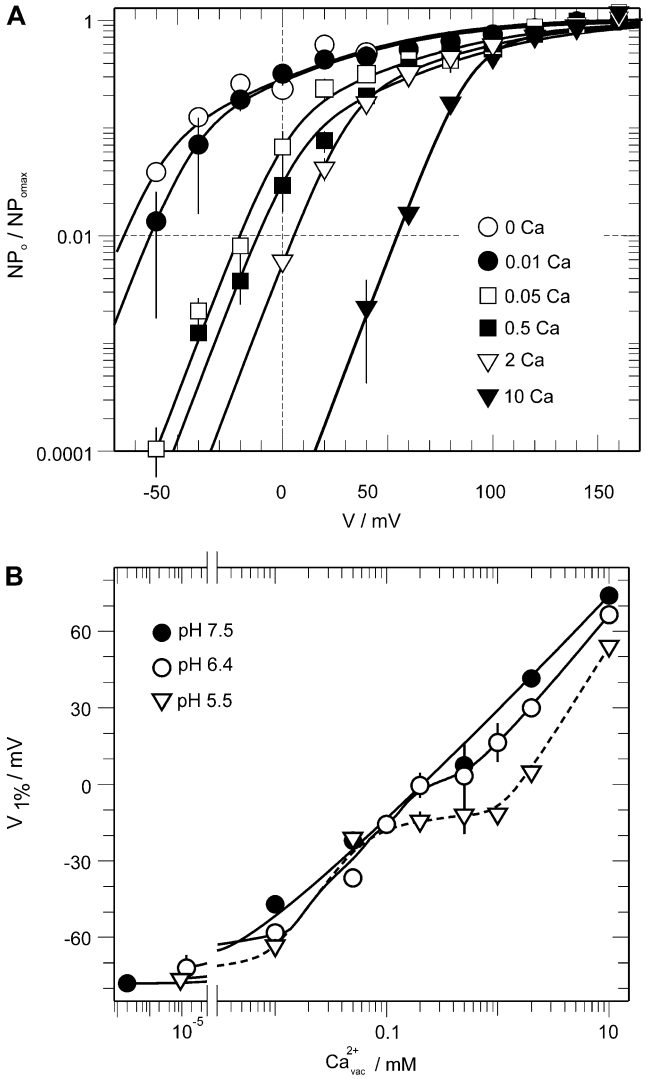


**Fig. 2.** Vacuolar pH modifies the dependence of the SV channel voltage activation on the vacuolar $Ca^{2+}$. (A) Voltage dependence of the SV channel activation at different vacuolar free $Ca^{2+}$ concentrations (indicated in mM at the right of the corresponding symbols) and pH 5.5. SV channel activity was analysed in large isolated tonoplast patches ($n$=4–8 patches for each $Ca^{2+}$ concentration, means ±SEM). Dashed horizontal line indicates the voltage at which 1% of maximum number of SV channels are open. (B) Dependence of the threshold for SV channel voltage activation (a membrane potential at which 1% of maximal number of SV channels are open) on the vacuolar free $Ca^{2+}$ at different vacuolar pH. Data for pH 7.5 were calculated from Pottosin *et al.* (2004). Solution composition was: symmetric 100 mM KCl; 2 mM free $Ca^{2+}$ at cytosolic side; cytosolic and vacuolar pH values were 7.5 and 5.5, respectively.

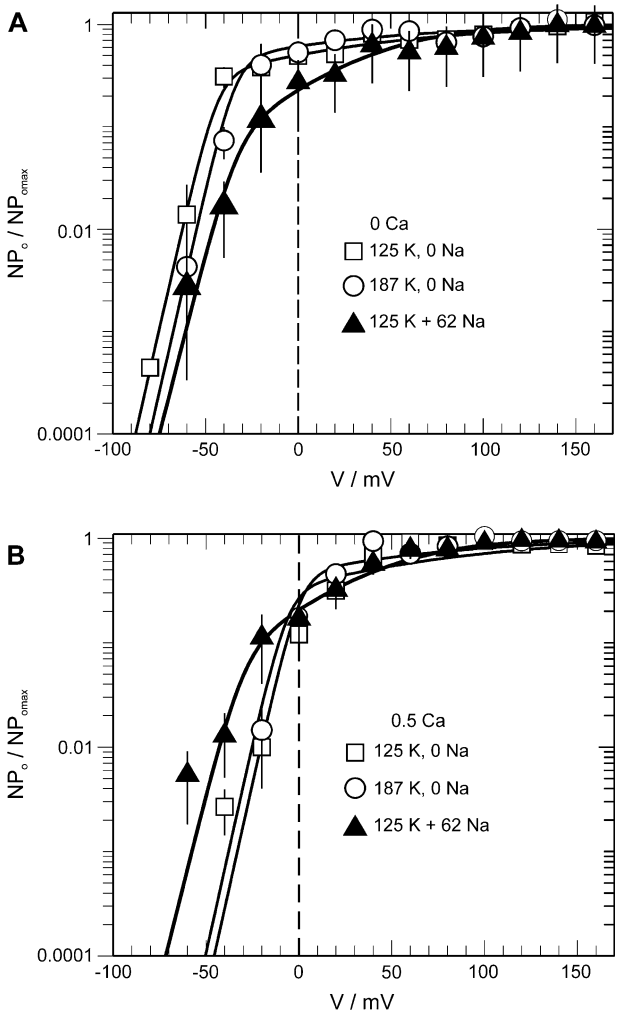


**Fig. 3.** Vacuolar $Na^+$ has opposite effects on the SV channel voltage dependence at zero and submillimolar vacuolar $Ca^{2+}$. Voltage dependence of the SV channel activity in large isolated tonoplast patches at two vacuolar free $Ca^{2+}$ concentrations, *c.* 10 nM (A) and 0.5 mM (B). Vacuolar $K^+$ and $Na^+$ concentrations (in mM) for each condition are indicated, 100 mM KCl, 2 mM free $Ca^{2+}$ (pH 7.5) at cytosolic side. Data are means ±SEM, $n$=3 patches for each condition.

channel voltage dependence and $V_{1\%}$ at zero vacuolar $Ca^{2+}$ (Fig. 2).

Sugar beet is a salt-tolerant species that uses $Na^+$ for maintaining cell turgor. Accordingly, the impact of vacuolar sap $Na^+$ on the voltage dependence of the SV channel at zero and 0.5 mM vacuolar $Ca^{2+}$ was verified (Fig. 3). At zero $Ca^{2+}$, addition of 62 mM $Na^+$ caused an increase in the voltage threshold of SV channel activation. This exceeded the effect of the addition of equimolar concentration of $K^+$ (Fig. 3A). However, in the presence of 0.5 mM $Ca^{2+}$ at the luminal side, addition of $Na^+$ resulted in the opposite effect, i.e. a decrease in the activation threshold (Fig. 3B). Alternatively, the results presented in Fig. 3 could be read in a different manner. Indeed, the activation curves are the same at zero and 0.5 mM $Ca^{2+}$ in the presence of $Na^+$, indicating that in the presence of 62 mM $Na^+$, a vacuolar $Ca^{2+}$ increase from zero to 0.5 mM does not have a significant impact on the SV channel voltage dependence. In other words, the presence of physiologically relevant $Na^+$ concentrations in cell vacuoles desensitizes the SV channel to vacuolar $Ca^{2+}$ variation between zero and 0.5 mM.

Finally, the modulation of the SV channel voltage dependence by vacuolar $Ca^{2+}$ at pH 5.5 in the presence of physiological concentrations of $K^+$, $Na^+$, and $Mg^{2+}$ was analysed. Addition of 62 mM $Na^+$ and 8 mM $Mg^{2+}$ to the vacuolar solution shifted the activation threshold at zero vacuolar $Ca^{2+}$ by ~35 mV to more positive potentials (Figs 4A, 2A). Also the threshold dependence on vacuolar $Ca^{2+}$ flattened: not only the $Ca^{2+}$change from 0.1 mM to 1 mM produced little change in the threshold but, in addition, the $Ca^{2+}$ increase from zero to 0.1 mM caused a lesser $V_{1\%}$ shift compared to the case without $Mg^{2+}$ and $Na^+$ at the luminal side (Fig. 4B). For comparison, threshold potentials were evaluated in vacuole-attached patches, with patch-pipettes filled with the standard cytosolic high $Ca^{2+}$ solution and variable free $Ca^{2+}$ in the bath. Threshold $V_{1\%}$ values (in mV) were as follows: $-14.4\pm0.1$, $-11.3\pm8.7$, $-14.9\pm7.4$, and $+5.3\pm0.3$ ($n$=4–5 vacuoles) using bath free $Ca^{2+}$ of 0, 0.1, 0.5, and 1 mM, respectively. Increased threshold at 1 mM free $Ca^{2+}$ in the bath probably reflects an increase of vacuolar $Ca^{2+}$, due to $Ca^{2+}$ ions entering the vacuole from the bath via open $Ca^{2+}$-activated SV channels. Indirect evidence that such a process takes place comes from the membrane potential measurements (Fig. 1C). At $[Ca^{2+}] \geqslant 1$ mM, the membrane potential became more sensitive to changes in bath $Ca^{2+}$, implying a larger contribution of the tonoplast $Ca^{2+}$-permeable channels. Providing at bath $Ca^{2+} < 1$ mM the vacuolar sap composition is unperturbed due to the exchange with the bath, the $V_{1\%}$ mean values for vacuole-attached patches would then be in the $-15$ mV to $-11$ mV range. These values can be compared with those obtained on excised patches at different vacuolar $Ca^{2+}$ levels, with the concentrations of other cations at the luminal side mimicking the vacuolar content. For excised patches $V_{1\%}$ values between $-15$ mV and $-11$ mV were obtained at vacuolar $Ca^{2+}$ levels between 0.1 mM and 0.7 mM (Fig. 4B). This is in a good agreement with a mean vacuolar free $Ca^{2+}$ activity ~0.2 mM reported by ion-selective microelectrodes (Table 2). Thus, in intact isolated vacuoles, the voltage-dependent activity of the SV channel is most likely controlled by a joint action of major vacuolar cations ($K^+$, $Na^+$, $Mg^{2+}$, $Ca^{2+}$) and pH.

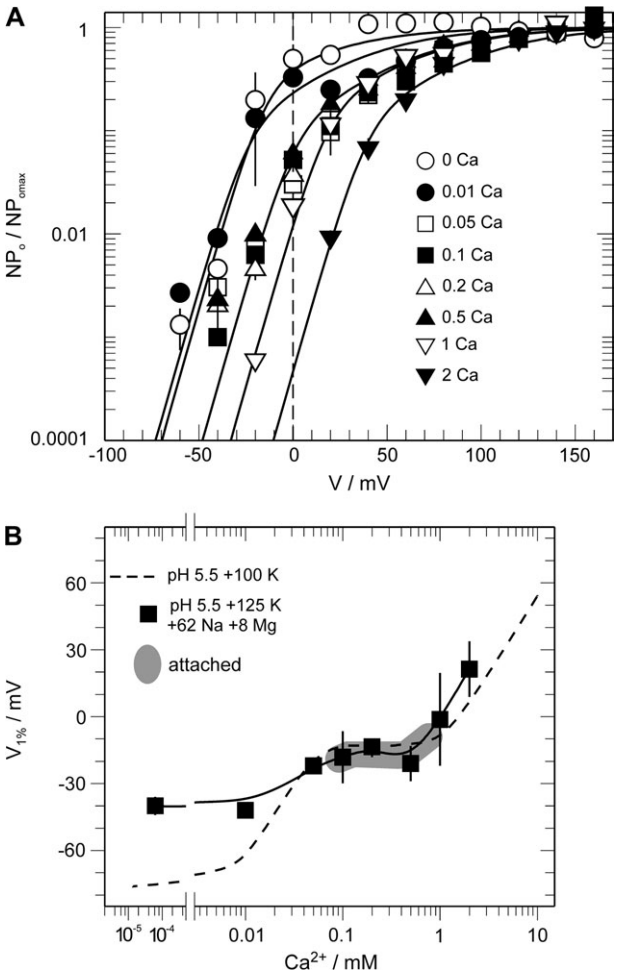


**Fig. 4.** The presence of various cations at the luminal side makes the SV channel almost insensitive to changes in vacuolar $Ca^{2+}$ from zero up to the millimolar range. (A) Voltage dependence of the SV channel activity in large isolated tonoplast patches at different vacuolar free $Ca^{2+}$ concentrations. The solution at the vacuolar side contained (in mM): 125 KCl, 62 NaCl, 8 $MgCl_2$ (pH 5.5), and at the cytosolic side: 100 mM KCl, 2 mM free $Ca^{2+}$ (pH 7.5). (B) Dependence of the threshold for SV channel voltage activation (membrane potential at which 1% of maximum number of SV channels are open) on the vacuolar free $Ca^{2+}$. Other components of the vacuolar and cytosolic solutions are as above. For comparison, a dependence obtained in 100 mM KCl (pH 5.5) was redrawn from Fig. 2B (dashed line). The range of values obtained in the attached patches is indicated (grey zone). Data are means ±SEM, $n$=3–5 patches for each condition.

### *The SV channel activity at low cytosolic $Ca^{2+}$*

All the results illustrated in Figs 2–4 were obtained at non-physiologically high cytosolic $Ca^{2+}$ concentrations (2 mM). Now, the SV channel voltage-dependent activity was analysed at lower cytosolic $Ca^{2+}$ (0.1–20 μM), in the presence of physiologically relevant concentrations of major cations and pH at the vacuolar side. The effects of increasing cytosolic $Mg^{2+}$ from 0.5 mM to 1.5 mM were also checked. Because at high positive potentials, huge SV channel-mediated currents from a typical vacuole tend to saturate the amplifier, small vacuolar vesicles with a visible diameter of 5–10 μm were isolated after achieving the whole vacuole configuration. The advantage of this compared to a standard outside-out configuration, is a larger current magnitude and a higher precision of measurement of the membrane capacitance (range 1–4 pF). This enabled the evaluation of the SV current per unit membrane area.

A typical example of the effect of cytosolic $Ca^{2+}$ and $Mg^{2+}$ variation on SV currents is illustrated in Fig. 5A. Both cations increase the SV current measured at high positive potentials. Titration curves for $Ca^{2+}$ at +100 and +180 mV

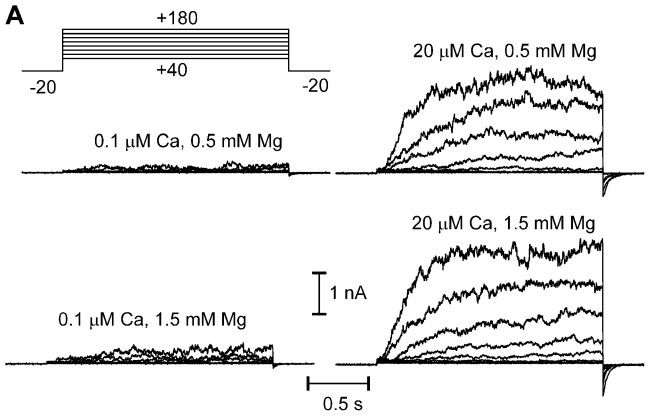


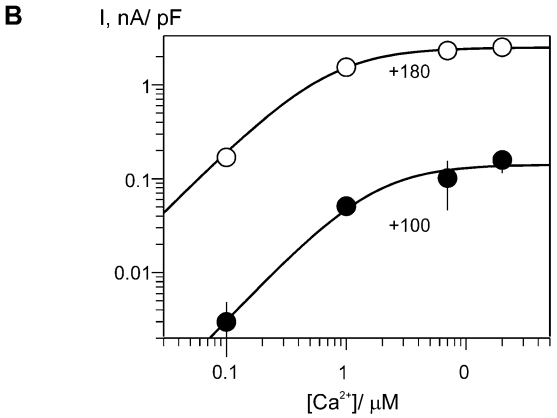


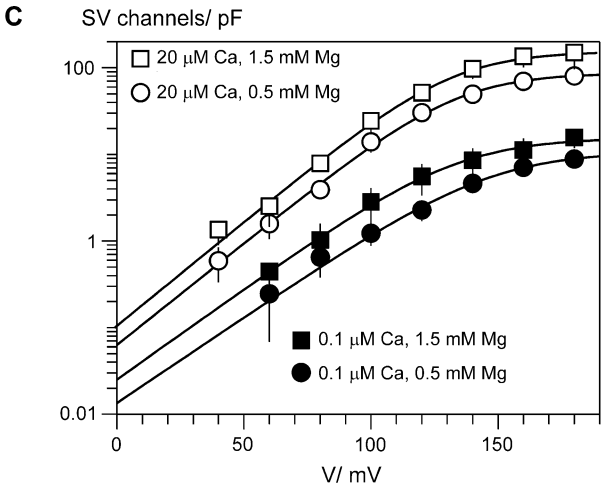


**Fig. 5.** Sensitivity of the SV channel to cytosolic $Ca^{2+}$ and $Mg^{2+}$ at physiological concentrations of vacuolar cations. (A) An example of a SV current record from a small ($c \sim 1$ pF) outside (cytosolic side)-out vesicle at different concentrations of cytosolic $Ca^{2+}$. External (cytosolic) solution contained 100 mM KCl (pH 7.4). The composition of a pipette (vacuolar) solution is as in Fig. 4. (B) The $Ca^{2+}$-dependence of the SV current (nA/pF) at +180 and +100 mV. Cytosolic free $Mg^{2+}$ was 0.5 mM, and other ionic conditions are as in (A). Data are presented as mean ±SEM ($n$=6–10 vacuoles). Solid lines are the best fits to the Hill equation, with $K_d$ for cytosolic $Ca^{2+}$ at 1.4±0.7 μM and 0.7±0.1 μM, and Hill coefficients of 1.4±0.2 and 1.3±0.2 for +100 and +180 mV, respectively. (C) Voltage dependence of the SV current at different cytosolic free $Ca^{2+}$ and $Mg^{2+}$ levels. A macroscopic SV current was divided by the single channel current at each potential and by membrane capacitance, yielding the mean number of the open channels per pF. Data are means ±SEM ($n$=4–8 vacuoles). Solid lines are the best fits to the Boltzmann equation with parameter values given in Table 3.

**Table 3.** *Parameters of the SV channel voltage dependence at different cytosolic $Ca^{2+}$ and $Mg^{2+}$*

| Cytosolic free $Ca^{2+}$ and $Mg^{2+}$ concentrations | Maximum open SV channels number | Gating charge (z) | Midpoint potential (mV) |
|---|---|---|---|
| Outside-outs | | | |
| 0.1 μM $Ca^{2+}$+0.5 mM $Mg^{2+}$ | 11±2/pF | 1.14±0.20 | 146±8 |
| 0.1 μM $Ca^{2+}$+1.5 mM $Mg^{2+}$ | 16±2/pF | 1.32±0.18 | 134±7 |
| 20 μM $Ca^{2+}$+0.5 mM $Mg^{2+}$ | 87±8/pF | 1.41±0.06 | 133±4 |
| 20 μM $Ca^{2+}$+1.5 mM $Mg^{2+}$ | 163±5/pF | 1.43±0.05 | 133±2 |
| Attached | | | |
| 0.1 μM $Ca^{2+}$+0.5 mM $Mg^{2+}$ | 4.2±0.5 | 1.18±0.06 | 136±6[a] |
| 20 μM $Ca^{2+}$+0.5 mM $Mg^{2+}$ | 44±1 | 1.32±0.15 | 96±3[a] |

[a] Potential values for the attached patches are referred to the command voltage and should be corrected for the resting tonoplast electric potential difference, ~+10 mV at these conditions.

yielded $K_d$ values of 1.4±0.7 μM and 0.7±0.1 μM, respectively (Fig. 5B), implying that cytosolic $Ca^{2+}$ binding is essentially voltage-independent. In addition, a detailed analysis of the voltage-dependence at 0.1 μM and 20 μM cytosolic $Ca^{2+}$ revealed only a small shift in the activation curve at 0.5 mM cytosolic $Mg^{2+}$, with no shift whatsoever at higher (1.5 mM) $Mg^{2+}$ (Fig. 5C; Table 3). Furthermore, the slope (determined by the gating charge, $z$) of voltage dependence increased only slightly upon the increase of cytosolic $Ca^{2+}$ from 0.1 μM to 20 μM (Table 3). Altogether, this suggests that the contribution of $Ca^{2+}$ binding from the cytosolic side to the SV channel voltage gating is insignificant. Increasing the cytosolic $Mg^{2+}$ concentration caused about a 2-fold stimulation of the SV channels. This effect was comparable at all membrane voltages and cytosolic $Ca^{2+}$ concentrations (Fig. 5; Table 3). Therefore, for this range of cytosolic free cation concentrations ($Ca^{2+}$: 0.1–20 μM, $Mg^{2+}$: 0.5–1.5 mM), divalent cations increase the mean number of voltage-activated SV channels without a substantial alteration of their voltage dependence. One may presume, however, that this does not remain true for higher cytosolic $Ca^{2+}$. The potential at which 1% of voltage-activated SV channels are open at 20 μM cytosolic $Ca^{2+}$ is about +48 mV (Fig. 5C). For a comparison, at very high (2 mM) cytosolic $Ca^{2+}$ and physiologic (0.2 mM) vacuolar $Ca^{2+}$ (Fig. 4B), the $V_{1\%}$ value was $\sim -15$ mV.

Finally, the voltage-dependent activity of the SV channel was analysed in vacuole-attached patches at high (20 μM) and low (0.1 μM) $Ca^{2+}$. As the membrane capacitance in these experiments was very low (<1 pF), its precise value could not be determined accurately. Thus,

the channel density could not be determined either. Instead, the mean number of open SV channels per patch was accessed as a function of membrane potential (Fig. 6; Table 3). The actual electric potential difference across a membrane patch in attached configuration is a sum of the resting trans-tonoplast potential and the command voltage. In a separate set of experiments, using small-tip patch-clamp pipettes filled with 3 M KCl the resting trans-tonoplast potential difference was determined. For bath solutions with 0.1 μM and 20 μM $Ca^{2+}$, resting potentials were +12±3 mV ($n$=11 vacuoles) and +9±2 mV ($n$=9), respectively. Such cytosolic-side positive potentials were due to the absence of $H^+$-pump activity. In the presence of 2 mM Mg-ATP, respective resting tonoplast potentials for 0.1 μM and 20 μM $Ca^{2+}$ baths became –4±2 mV ($n$=11) and –12±4 mV ($n$=11), respectively.

Correcting the membrane voltage in attached patches for a resting potential difference, the parameters of the SV channel voltage dependence in attached and excised (outside-out) patches became identical at low (0.1 μM) cytosolic $Ca^{2+}$ (Table 3). However, in contrast to outside-out patches, increasing the cytosolic $Ca^{2+}$ from 0.1 μM to 20 μM caused a relatively large (40 mV; Table 3) shift of the voltage dependence to more negative potentials. Further on, the 1% voltage threshold (corrected for the resting potential) was about +20 mV for attached patches at 20 μM cytosolic $Ca^{2+}$, compared to the −5 to −25 mV range obtained for vacuolar-attached patches facing very high (2 mM) cytosolic $Ca^{2+}$ (Fig. 4B).

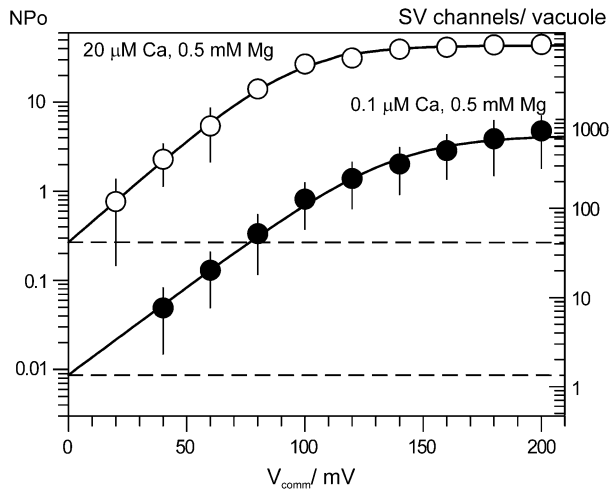


**Fig. 6.** Slow-vacuolar channel activity in vacuole-attached patches. Bath and pipette solutions are identical, 100 mM KCl (pH 7.4) and free $Ca^{2+}$ and $Mg^{2+}$ concentrations are as indicated at the top of the curves. A macroscopic SV current was divided by the single channel current at each potential, yielding the mean number of open channels per patch (NPo). For comparison, assuming the same channel density as in outside-out patches (Fig. 5), the mean open SV channel number per typical vacuole of 50 μm diameter is given at the second $y$-axis on the right. Data are means ±SEM ($n$=4). Solid lines are the best fits to the Boltzmann equation with parameter values given in Table 3. Voltages were command potentials for this case; to convert them to the actual tonoplast electric potential difference, the resting potential value (about +10 mV at these conditions, as verified by 3 M KCl-filled microelectrode impalements) should be totalled.

## Discussion

### *Other vacuolar cations desensitize the SV channel to changes in luminal $Ca^{2+}$*

In this study, the free vacuolar concentrations of all major physiological cations were determined (Table 2). To our knowledge, this is the first report of free vacuolar $Mg^{2+}$ concentrations in higher plants. In addition, using two independent approaches, it was found that the mean free vacuolar $Ca^{2+}$ concentration in *Beta* taproots was ~0.2 mM, an order of magnitude lower than previously reported values for *Zea* roots and *Riccia* rhizoids (Felle, 1988). Therefore, a re-evaluation of the modulation of SV channel activity by vacuolar $Ca^{2+}$ under more realistic vacuolar cation concentrations and pH is required.

Our main findings can be summarized as follows: in the presence of cations other than $Ca^{2+}$ at their physiological concentrations and at acidic pH inside the vacuole, the SV channel voltage-dependent activity becomes insensitive to vacuolar $Ca^{2+}$ variation within the physiological range (Fig 4B). Part of this effect is non-specific and related to the screening of the negative charge at the membrane surface, thus reducing vacuolar $Ca^{2+}$ binding at high ionic strength (Pottosin *et al.*, 2005). However, some monovalent cations such as $Na^+$ and $Cs^+$ appear to exert specific effects on the SV channel voltage dependence when compared to $K^+$ (Ivashikina and Hedrich, 2005; Ranf *et al.*, 2008). The $Na^+$-induced shift in the SV channel voltage dependence found here is comparable to that reported by Ivashikina and Hedrich (2005) at similar (zero vacuolar $Ca^{2+}$) conditions. However, in a background of more realistic vacuolar $Ca^{2+}$ concentrations (0.5 mM in our case), $Na^+$ caused an opposite shift (Fig. 3B). Therefore, accumulation of $Na^+$ in the vacuole during salt stress could ameliorate the inhibitory effects of vacuolar $Ca^{2+}$ on the SV channel.

The effect of vacuolar $Mg^{2+}$ was qualitatively similar to that of $Ca^{2+}$, but smaller in magnitude (Pottosin *et al.*, 2004). However, bearing in mind the much higher vacuolar $Mg^{2+}$ concentration compared to that of $Ca^{2+}$ (Table 3), the actual effects of these two ions on the SV channel voltage dependence may be comparable.

In a previous study (Pottosin *et al.*, 2004), a detailed kinetic model of stabilization of the closed states of the SV channel by vacuolar $Ca^{2+}$ and $Mg^{2+}$ was generated. In particular, it was found that up to three $Ca^{2+}$ or $Mg^{2+}$ ions could be bound in one of the closed states: C2. For simplicity, it was proposed that divalent cation binding at this state was non-co-operative and occurred with the same $K_d$ values. In the present work it is demonstrated

that, at acidic pH, the dependence of the activation threshold on vacuolar $Ca^{2+}$ (reflecting mainly the stabilization of C2-state by $Ca^{2+}$) becomes complex, with a distinct plateau in a physiological $Ca^{2+}$ range (Fig. 2B).

Curiously, protons by themselves do not affect SV channel voltage dependence at zero vacuolar $Ca^{2+}$. This may be due to the fact that vacuolar protons bind with equal p*K*s in closed and open states, so not affecting the distribution between states at any voltage. However, $H^+$ binding obviously affects the vacuolar $Ca^{2+}$ binding. The effect of acidic pH presented in Fig. 2B may be explained for example, if the protonation of the SV channel protein results in a much higher $K_d$ for binding of the second and third $Ca^{2+}$ ions. Therefore, a plateau between 0.1 mM and 1 mM $Ca^{2+}$ may reflect the saturation of the first $Ca^{2+}$ ion binding in all states. [At these $Ca^{2+}$ concentrations, in accordance with $K_d$ values for a single $Ca^{2+}$ ion binding from Pottosin *et al.* (2004), all states (open and two closed: C1 and C2) will contain a bound $Ca^{2+}$ ion. Hence, further stabilization of closed states and respective voltage threshold shift is only possible with binding of extra $Ca^{2+}$ ions to the C2-state.] It should be noted though, that the effects of different cations are not additive. Rather, it seems that they compete with $Ca^{2+}$ binding, thus diminishing the modulation effect of $Ca^{2+}$ on the SV channel.

Our working hypothesis therefore, is that the existence of diverse modulatory effects exerted by multiple cations in the vacuolar lumen assists in 'buffering' the SV channel activity. Consequently, the variation of vacuolar concentration of a single component, even one as powerful as $Ca^{2+}$, would not result in a large shift in the SV channel voltage dependence.

### *The SV channel activity at resting trans-tonoplast potentials*

In the absence of externally applied voltage and at resting cytosolic $Ca^{2+}$ (100 nM), on average 0.01 SV channels per patch will be open, as judged by the activation curve shown for vacuole-attached patches (Fig. 6). This is equivalent to 0.023% of the number of channels open at 20 μM cytosolic $Ca^{2+}$ and high membrane potentials. Assuming the same channel density as in outside-out patches (see Fig. 5C, 1 pF approximately corresponds to a 100 $\mu m^2$ membrane area), for a typical vacuole of 50 μm diameter or 7855 $\mu m^2$ membrane surface area, as an average only 1.5 SV channels per vacuole will be open at any time. At 20 μM cytosolic $Ca^{2+}$, about 40 SV channels per vacuole will be open at resting potentials (Fig. 6), and this can be taken as an upper estimate (see the dose dependence in Fig. 5B).

The properties of $Ca^{2+}$ fluxes reported by the MIFE technique, their stimulation by $Mg^{2+}$ and a strong inhibition by $Zn^{2+}$, suggests that they are mediated by SV channels. Moreover, the $Ca^{2+}$ release from isolated beet vacuoles, similar to the SV current, was stimulated by cytosolic $Ca^{2+}$, reaching a maximum of $2.8\pm0.6$ nmol $m^{-2}$ $s^{-1}$ (Fig. 1) at 20 μM cytosolic $Ca^{2+}$. Assuming a 50 μm vacuole diameter, this equates to a current of $4.3\pm0.9$ pA per vacuole. Comparison of the $Ca^{2+}$ flux magnitude and the number of open SV channels at 20 μM cytosolic $Ca^{2+}$, suggests that each SV channel mediates a net $Ca^{2+}$ current of ~100 fA at the resting trans-tonoplast potential. This value fits remarkably well the theoretical predictions for *Beta* SV channel: 100–120 fA of the $Ca^{2+}$ current per channel at zero voltage, weakly sensitive to *p*Ca for a physiological range of $Ca^{2+}$ gradients (Gradmann *et al.*, 1997).

In reality, SV-mediated $Ca^{2+}$ release could be even smaller. Indeed, the resting potential of the isolated vacuoles in our experiments were depolarized (~+10 mV for cytosolic bath with 0.1–20 μM $Ca^{2+}$ plus 0.66 mM $Mg^{2+}$) in the absence of substrates for vacuolar $H^+$ pumps. The addition of 2 mM Mg-ATP into the bath solutions resulted in more negative membrane potential values, –4 to –12 mV. This is comparable to directly measured values for the tonoplast in intact barley roots and leaves, −10 to −15 mV and ~0 mV, respectively (Walker *et al.*, 1996; Cuin *et al.*, 2003). An even lower negative value of −30 mV was reported for Arabidopsis leaves (Miller *et al.*, 2001). Based on the parameters values for the SV voltage dependence (Table 3), a negative shift of membrane potential by 16–21 mV results in a 2–3 times lower SV channel activity. However, a more negative potential implies an increase in a driving force (resting potential *minus* $E_{Ca}$) for vacuolar $Ca^{2+}$ release. For 20/200 μM $Ca^{2+}$ gradient the relative increase in the $Ca^{2+}$ driving force is significant, from –20 mV in the absence of ATP to –41 mV in the presence of 2 mM Mg-ATP (negative sign implies the preferential $Ca^{2+}$ influx to the cytosol from the vacuole). Bearing in mind that $Ca^{2+}$ flux under asymmetric conditions is not linear and displays an inward rectification (increase of chord conductance when the potential difference between cytosol and vacuole is made more negative) (Gradmann *et al.*, 1997), one may expect that at resting tonoplast potential $Ca^{2+}$ flux through an open SV channel will increase more than the increase in driving force, i.e. >2 times. Therefore, at high (e.g. 20 μM) cytosolic $Ca^{2+}$ the decrease of the SV channel open probability will be almost compensated by the increase of $Ca^{2+}$ flux through a single channel. At low cytosolic $Ca^{2+}$ the relative change of $Ca^{2+}$ driving force due to a negative shift of resting tonoplast potential will be less significant. Therefore, total $Ca^{2+}$ release from the vacuole will be reduced in this case, due to a decrease in the mean number of open SV channels.

The cytosolic $Ca^{2+}$ level of 20 μM considered above may lead to another overestimate of the SV channel activity. Under physiological ionic conditions, half-activation of

the SV channel occurs at 0.7–1.4 μM cytosolic $Ca^{2+}$ (Fig. 5B), close to $K_d$=1.5 μM defined by Hedrich and Neher (1987). These values are near the peak global free $Ca^{2+}$ levels reached during plant responses to several abiotic stresses (Ranf *et al*., 2008). Thus, the overestimation will be approximately 2-fold. For isolated vacuoles, the SV-mediated $Ca^{2+}$ release will come closer to that measured by the MIFE technique in the absence of added $Ca^{2+}$: 1 nmol $m^{-2}$ $s^{-1}$ or 1.5 pA per vacuole.

Considering therefore both the more negative trans-tonoplast potential and lower cytosolic $Ca^{2+}$, the whole vacuole population of SV channels would produce a global $Ca^{2+}$ release into the cytosol of ⩽1 pA. Assuming that for a typical cell the vacuole and the cytosol occupy 80% and 20% of the volume, respectively, and that a vacuole has a diameter of 50 μm, cytosolic volume will be ~16 pl. Therefore, net cytosol-directed $Ca^{2+}$ current of 1 pA will tend to change the *total* cytosolic $Ca^{2+}$ concentration at 35 μM $min^{-1}$ rate. However, cytosolic $Ca^{2+}$ is strongly buffered. For plant cells, the estimated buffering capacity $B_{max}$ is 0.2–0.5 mM (Trewavas, 1999) whereas the effective dissociation constant $K_d$ for a cytosolic $Ca^{2+}$ buffer in different cell types ranges between 0.15 μM and 0.6 μM (Martinez-Serrano *et al*., 1992; Kuratomi *et al*., 2003). Assuming a simple Michaelis–Menten behaviour, the relation between total and free cytosolic $Ca^{2+}$ may be expressed as $1 + B_{max}/(Ca_{free} + K_d)$. Therefore, when free cytosolic $Ca^{2+}$ approaches the $K_d$, about 1 out of 500 $Ca^{2+}$ ions as an average could be found in the free form. Thus, the SV channel mediated increase of *free* cytosolic $Ca^{2+}$ would be ⩽70 nM $min^{-1}$, which is by several orders of magnitude slower than the $Ca^{2+}$ responses to most abiotic stresses, and still slower than elicitor-induced $Ca^{2+}$ signals (Ranf *et al*., 2008). Yet, as discussed below, in intact cells the SV channel reactivity could be locally increased due to the formation of a high $Ca^{2+}$ microdomain resulting from channel gathering, as well as tight contact with $Ca^{2+}$-permeable channels located at other membranes.

Thus, SV channels make little, if any contribution to *global* cytosolic $Ca^{2+}$ responses, as convincingly demonstrated in a recent study by Ranf *et al*. (2008). This result is expected and perfectly reasonable in view of the fact that the vacuole is an inexhaustible $Ca^{2+}$ store. Hence, the analogy with the CICR in animal cells may be not valid, because the latter phenomenon is assigned to a different $Ca^{2+}$ store, such as the endoplasmic reticulum (ER) that can be readily and reversibly depleted. In contrast to the small-sized ER store, depleting a large vacuole, which can occupy up to 90% of the plant cell volume, will inevitably cause irreversible alterations in the cytosolic $Ca^{2+}$. Therefore, although the activation of SV channels by cytosolic $Ca^{2+}$ provides a positive feedback system, i.e. the more $Ca^{2+}$ released via the SV channel, the higher the activity of this and neighbouring SV channels, a strict negative SV channel control by physiological factors (see Pottosin and Schönknecht, 2007, for more details) effectively prevents this chain reaction at the whole cell level.

As Ranf *et al*. (2008) used a cytosolic aequorin reporter, their data set aside the potential role of the SV channel in local $Ca^{2+}$ signalling, because this could not be detected by their method. Such local $Ca^{2+}$ signals, the so-called $Ca^{2+}$ sparks and puffs, have been well studied in animal cells. For instance, in tight junctions of striated muscle, a cross-talk between sarcoplasmic ryanodine receptor channels (RyRs) and voltage-dependent $Ca^{2+}$ channels of t tubules is initiated. This occurs due to a clustering of RyRs and their positive regulation by cytosolic $Ca^{2+}$, thereby generating a synchronous response of several RyRs: a $Ca^{2+}$ spark (Franzini-Armstrong and Protasi, 1997). It should be noted that, with respect to high $Ca^{2+}$ microdomains, a free $Ca^{2+}$ concentration at a distance of ~0.1 μm from the pore entrance of a $Ca^{2+}$ conducting channel may reach the hundred micromole range (Demuro and Parker, 2006; Rizutto and Pozzan, 2006). Due to its vast area, the tonoplast is often in contact with several intracellular stores, as well as the plasma membrane. Furthermore, tonoplast SV channels are very abundant. Based on the surface density (Fig. 5C), the average distance between neighbouring channels is less than 1 μm. Thus, there should almost certainly be several SV channel copies in the contact zones of the tonoplast with other membranes. Provided the SV channels are clustered so as to increase the cross-activation by $Ca^{2+}$ ions released from the vacuole into the cytosol, and that at least one channel of each cluster is at a short (~100 nm) distance from a $Ca^{2+}$-permeable channel of another membrane (e.g. plasma- or ER membrane), the conditions for $Ca^{2+}$ spark formation will be met. Therefore, a functionally large vacuole would be split in multiple small circuits, and the vacuolar $Ca^{2+}$ release would be asynchronous and restricted to local contact zones with other organelles and the plasma membrane. This hypothesis should be addressed in further studies employing such techniques as high-resolution confocal or TIRF microscopy on intact cells (Demuro and Parker, 2006).

In conclusion, a combination of MIFE $Ca^{2+}$ flux measurements and patch-clamp evaluations of the SV channel activity in isolated vacuoles suggests that only a minor contribution to global $Ca^{2+}$ signalling is made by SV channel-mediated vacuolar $Ca^{2+}$ release. Whether the vacuolar SV channels are capable of modulating local $Ca^{2+}$ responses remains to be elucidated.

## Acknowledgements

This study was supported by CONACyT project 38181N to IP, VP received the fellowship from the same project. ARC funding to SS is gratefully acknowledged. The authors are indebted to Dr TA Cuin for a critical review of the paper.

## References


**Allen GJ, Sanders D, Gradmann D.** 1998. Calcium–potassium selectivity: kinetic analysis of current–voltage relationships of the open, slowly activating channel in the vacuolar membrane of *Vicia faba* guard-cells. *Planta* **204,** 528–541.

**Carpaneto A, Cantu AM, Gambale F.** 2001. Effects of cytoplasmic $Mg^{2+}$ on slowly activating channels in isolated vacuoles of *Beta vulgaris*. *Planta* **213,** 457–468.

**Carter C, Pan S, Zouhar J, Avila EL, Girke T, Raikhel NV.** 2004. The vegetative vacuole proteome of *Arabidopsis thaliana* reveals predicted and unexpected proteins. *The Plant Cell* **16,** 3285–3303.

**Chen Z, Newman I, Zhou M, Mendham N, Zhang G, Shabala S.** 2005. Screening plants for salt tolerance by measuring $K^+$ flux: a case study for barley. *Plant, Cell and Environment* **28,** 1230–1246.

**Cuin TA, Miller AJ, Laurie SA, Leigh RA.** 2003. Potassium activities in cell compartments of salt-grown barley leaves. *Journal of Experimental Botany* **54,** 657–661.

**Demuro A, Parker I.** 2006. Imaging single-channel calcium microdomains. *Cell Calcium* **40,** 413–422.

**Felle H.** 1988. Cytoplasmic free calcium in *Riccia fluitans* L. and *Zea mays* L.: interaction of $Ca^{2+}$ and pH? *Planta* **176,** 248–255.

**Franzini-Armstrong C, Protasi F.** 1997. Ryanodine receptors of striated muscles: a complex channel capable of multiple interactions. *Physiological Reviews* **77,** 699–729.

**Gambale F, Cantu' AM, Carpaneto A, Keller BU.** 1993. Fast and slow activation of voltage-dependent ion channels in radish vacuoles. *Biophysical Journal* **65,** 1837–1843.

**Gradmann D, Johannes E, Hansen U-P.** 1997. Kinetic analysis of $Ca^{2+}/K^+$ selectivity of an ion channel by single-binding-site models. *Journal of Membrane Biology* **159,** 169–178.

**Hedrich R, Barbier-Brygoo H, Felle H, *et al.*** 1988. General mechanisms for solute transport across the tonoplast of plant vacuoles: a patch-clamp survey of ion channels and proton pumps. *Botanica Acta* **101,** 7–13.

**Hedrich R, Kurkdjian A.** 1988. Characterization of an anion-permeable channel from sugar beet vacuoles: effects of inhibitors. *The EMBO Journal* **7,** 3661–3666.

**Hedrich R, Neher E.** 1987. Cytoplasmic calcium regulates voltage-dependent ion channels in plant vacuoles. *Nature* **329,** 833–835.

**Ivashikina N, Hedrich R.** 2005. $K^+$ currents through SV-type vacuolar channels are sensitive to elevated luminal sodium levels. *The Plant Journal* **41,** 606–614.

**Kuratomi S, Matsuoka S, Sarai N, Powell T, Noma A.** 2003. Involvement of $Ca^{2+}$ buffering and $Na^+/Ca^{2+}$ exchange in the positive staircase of contraction in guinea-pig ventricular myocytes. *Pflügers Archiv—European Journal of Physiology* **446,** 347–355.

**Martinez-Serrano A, Blanco P, Satrústegui J.** 1992. Calcium binding to cytosol and calcium extrusion mechanisms in intact synaptosomes and their alterations with aging. *Journal of Biological Chemistry* **267,** 4672–4679.

**Miller AJ, Cookson SJ, Smith SJ, Wells DM.** 2001. The use of microelectrodes to investigate compartmentation and the transport of metabolized inorganic ions in plants. *Journal of Experimental Botany* **52,** 541–549.

**Newman IA.** 2001. Ion transport in roots: measurement of fluxes using ion-selective microelectrodes to characterize transporter function. *Plant, Cell and Environment* **24,** 1–14.

**Pei ZM, Ward JM, Schroeder JI.** 1999. Magnesium sensitizes slow vacuolar channels to physiological cytosolic calcium and inhibits fast vacuolar channels in fava bean guard cell vacuoles. *Plant Physiology* **121,** 977–986.

**Peiter E, Maathuis FJM, Mills LN, Knight H, Pelloux J, Hetherington AM, Sanders D.** 2005. The vacuolar $Ca^{2+}$-activated channel TPC1 regulates germination and stomatal movement. *Nature* **434,** 404–408.

**Pottosin II , Dobrovinskaya OR, Muñiz J.** 2001. Conduction of monovalent and divalent cations in the slow vacuolar channel. *Journal of Membrane Biology* **181,** 55–65.

**Pottosin II , Martínez-Estévez M, Dobrovinskaya OR, Muñiz J.** 2005. Regulation of the slow vacuolar channel by luminal potassium: role of surface charge. *Journal of Membrane Biology* **205,** 103–111.

**Pottosin II , Martínez-Estévez M, Dobrovinskaya OR, Muñiz J, Schönknecht G.** 2004. Mechanism of luminal $Ca^{2+}$ and $Mg^{2+}$ action on the vacuolar slowly activating channels. *Planta* **219,** 1057–1070.

**Pottosin II , Schönknecht G.** 2007. Vacuolar calcium channels. *Journal of Experimental Botany* **58,** 1559–1569.

**Pottosin II , Tikhonova LI, Hedrich R, Schönknecht G.** 1997. Slowly activating vacuolar channels can not mediate $Ca^{2+}$-induced $Ca^{2+}$ release. *The Plant Journal* **12,** 1387–1398.

**Ranf S, Wünnenberg P, Lee J, Becker D, Dunkel M, Hedrich R, Scheel D, Dietrich P.** 2008. Loss of the vacuolar cation channel, AtTPC1, does not impair $Ca^{2+}$ signals induced by abiotic and biotic stresses. *The Plant Journal* **53,** 287–299.

**Rizzuto R, Pozzan T.** 2006. Microdomains of intracellular $Ca^{2+}$: molecular determinants and functional consequences. *Physiological Reviews* **86,** 369–408.

**Schulz-Lessdorf B, Hedrich R.** 1995. Protons and calcium modulate SV-type channels in the vacuolar-lysosomal compartment. Channel interaction with calmodulin inhibitors. *Planta* **197,** 655–671.

**Trewavas A.** 1999. Le calcium, c'est la vie: calcium makes waves. *Plant Physiology* **120,** 1–6.

**Walker DJ, Leigh RA, Miller AJ.** 1996. Potassium homeostasis in vacuolate plant cells. *Proceedings of the National Academy of Sciences, USA* **93,** 10510–10514.

**Ward JM, Schroeder JI.** 1994. Calcium-activated $K^+$ channels and calcium-induced $Ca^{2+}$ release by slow vacuolar ion channels in guard cell vacuoles implicated in the control of stomatal closure. *The Plant Cell* **6,** 669–683.

**Wherrett T, Ryan PR, Delhaize E, Shabala S.** 2005. Effect of aluminium on membrane potential and ion fluxes at the apices of wheat roots. *Functional Plant Biology* **32,** 199–208.